# Vascular smooth muscle cell mechanotransduction through serum and glucocorticoid inducible kinase-1 promotes interleukin-6 production and macrophage accumulation in murine hypertension

Mario Figueroa, MD,[a] SarahRose Hall, BS,[a] Victoria Mattia, BS,[a] Alex Mendoza, BS,[a] Adam Brown, BS,[a] Ying Xiong, PhD,[b] Rupak Mukherjee, PhD,[b] Jeffrey A. Jones, PhD,[b,c] William Richardson, PhD,[d] *and* Jean Marie Ruddy, MD,[a,c] *Charleston, SC; and Fayetteville, AK*

## ABSTRACT

**Objective:** The objective of this investigation was to demonstrate that in vivo induction of hypertension (HTN) and in vitro cyclic stretch of aortic vascular smooth muscle cells (VSMCs) can cause serum and glucocorticoid-inducible kinase (SGK-1)-dependent production of cytokines to promote macrophage accumulation that may promote vascular pathology.

**Methods:** HTN was induced in C57Bl/6 mice with angiotensin II infusion (1.46 mg/kg/day × 21 days) with or without systemic infusion of EMD638683 (2.5 mg/kg/day × 21 days), a selective SGK-1 inhibitor. Systolic blood pressure was recorded. Abdominal aortas were harvested to quantify SGK-1 activity (pSGK-1/SGK-1) by immunoblot. Flow cytometry quantified the abundance of $CD11b^{+}/F480^{+}$ cells (macrophages). Plasma interleukin (IL)-6 and monocyte chemoattractant protein-1 (MCP-1) was assessed by enzyme-linked immunosorbent assay. Aortic VSMCs from wild-type mice were subjected to 12% biaxial cyclic stretch (Stretch) for 3 or 12 hours with or without EMD638683 (10 μM) and with or without SGK-1 small interfering RNA with subsequent quantitative polymerase chain reaction for IL-6 and MCP-1 expression. IL-6 and MCP-1 in culture media were analyzed by enzyme-linked immunosorbent assay. Aortic VSMCs from $SGK\text{-}1^{flox+/+}$ mice were transfected with Cre-Adenovirus to knockdown SGK-1 (SGK-1KD VSMCs) and underwent parallel tension experimentation. Computational modeling was used to simulate VSMC signaling. Statistical analysis included analysis of variance with significance at a $P$ value of $<.05$.

**Results:** SGK-1 activity, abundance of $CD11b^{+}/F4\text{-}80^{+}$ cells, and plasma IL-6 were increased in the abdominal aorta of mice with HTN and significantly reduced by treatment with EMD638683. This outcome mirrored the increased abundance of IL-6 in media from Stretch C57Bl/6 VSMCs and attenuation of the effect with EMD638683 or SGK-1 small interfering RNA. C57Bl/6 VSMCs also responded to Stretch with increased MCP-1 expression and secretion into the culture media. Further supporting the integral role of mechanical signaling through SGK-1, target gene expression and cytokine secretion was unchanged in SGK-1KD VSMCs with Stretch, and computer modeling confirmed SGK-1 as an intersecting node of signaling owing to mechanical strain and angiotensin II.

**Conclusions:** Mechanical activation of SGK-1 in aortic VSMCs can promote inflammatory signaling and increased macrophage abundance, therefore this kinase warrants further exploration as a pharmacotherapeutic target to abrogate hypertensive vascular pathology. (JVS—Vascular Science 2023;4:100124.)

**Clinical Relevance:** Only approximately 30% of patients with hypertension reach designated blood pressure goals through medical therapy, and even those who successfully obtain normotension will still have vascular functional abnormalities such as aortic stiffening, a known predictor of cardiovascular morbidity and mortality. Tension-induced aortic pathologies may be driven by inflammatory cell infiltration with dysfunctional matrix remodeling, suggesting that interruption of cardiovascular mechanotransduction may represent a complementary treatment pathway in hypertension. This study demonstrates that the serum and glucocorticoid-inducible kinase-1 is a vital mechanosensitive kinase within the aortic wall to promote inflammatory cell infiltration that may contribute to vascular pathology.

**Keywords:** Interleukin-6; Hypertension; Serum and glucocorticoid-inducible kinase-1 (SGK-1)

From the Division of Vascular Surgery,[a] and Division of Cardiothoracic Surgery,[b] Medical University of South Carolina, Charleston; the Ralph H. Johnson VA Medical Center, Charleston[c]; and the Department of Chemical Engineering, University of Arkansas, Fayetteville.[d]

Funded by T32 AR50958-17 to M.F.; Augusta University Medical Scholars Program 2021 to A.M.; Society for Vascular Surgery Student Research Fellowship 2021 to A.B.; VA Merit Award I01BX000904-08A1 to J.A.J.; and 1K08HL143169-01A1 to J.M.R.

Correspondence: Jean Marie Ruddy, MD, Associate Professor of Surgery, Division of Vascular Surgery, Medical University of South Carolina, 30 Courtenay Dr, MSC 295 Ste 654, Charleston, SC 29425 (e-mail: ruddy@musc.edu).

The editors and reviewers of this article have no relevant financial relationships to disclose per the JVS-Vascular Science policy that requires reviewers to decline review of any manuscript for which they may have a conflict of interest.

2666-3503



https://doi.org/10.1016/j.jvssci.2023.100124

In hypertension (HTN), the aorta is subject to shear stress and elevated wall tension that has been associated with dysfunctional remodeling, stiffening, and increased cardiovascular mortality.[1,2] Human samples, as well as animal models, have demonstrated leukocyte infiltration in hypertensive vascular disease.[3] The question of whether the wall stress caused by these hemodynamic forces is a product of the inflammatory infiltrate or if it contributes to the propagation of detrimental inflammatory signaling cascades remains unanswered. This laboratory has previously demonstrated that interleukin-6 (IL-6) and monocyte chemoattractant protein-1 (MCP-1) expression were elevated in murine aortic vascular smooth muscle cells (VSMCs) under conditions of biaxial stretch; interestingly, transcriptional activity was not enhanced by concurrent treatment with the vasoactive peptide angiotensin II (AngII).[4] Targeted interruption of this mechanical signal transduction may represent an opportunity to quench dysfunctional vascular remodeling.

With a focus on identifying the tension-induced pathway implicated in propagating hypertensive proinflammatory signaling, it was noted that the serum and glucocorticoid-inducible kinase-1 (SGK-1) has already demonstrated mechanosensitivity in other vascular beds such as vein bypass grafts.[5] Furthermore, in pulmonary HTN, blockade of SGK-1 improved pressure differentials and reduced macrophage infiltration.[6,7] Current evidence relating SGK-1 activity to systemic HTN has focused on renal ion channel production and function in salt-induced models,[8] such that knockout animals were protected from blood pressure elevation and consequential inflammation.[9,10] Regarding the intrinsic aortic cell response to tension, use of the AngII-induced murine HTN model has advantageous clinical translation, and infusion of that biologic stressor has likewise demonstrated the aorta as a specific target of damage and inflammation under conditions of HTN.[11] SGK-1 activity within the aortic wall of AngII-induced HTN has not been described and represents an opportunity to investigate the integrated biological and mechanical signaling pathways in HTN. Accordingly, this study focused on further specifying the role of SGK-1 in hypertensive vascular pathology by hypothesizing that SGK-1 activity is upregulated under conditions of elevated tension to promote proinflammatory cytokine production and macrophage accumulation.

## ARTICLE HIGHLIGHTS

- **Type of Research**: Basic and translational science
- **Key Findings:** Mechanical activation of the serum and glucocorticoid-inducible kinase-1 in the aortic wall during hypertension can increase proinflammatory signals from vascular smooth muscle cells that promote macrophage accumulation as potential key contributors to vascular pathology.
- **Take Home Message:** Mechanical activation of serum and glucocorticoid-inducible kinase-1 in aortic vascular smooth muscle cells can promote inflammatory signaling and increased macrophage abundance; therefore, this kinase warrants further exploration as a pharmacotherapeutic target to abrogate hypertensive aortic pathology.

## METHODS

**Animal care and use.** All animal care and surgical procedures were approved by the Medical University of South Carolina Institutional Animal Care and Use Committee (AR#2020-01,502). C57Bl/6 mice were purchased from Jackson Laboratories (Bar Harbor, ME). SGK-1$^{flox+/flox+}$ mice on a C57Bl/6 background were obtained from the Fejes-Toth laboratory (Dartmouth College, Hanover, NH).[12] Local breeding colonies were maintained. Although the study was not powered to detect sex-based differences, both male and female mice (12-20 weeks of age) were equally used in the experiment.

**AngII-induced HTN and SGK-1 inhibition with EMD638683.** AngII was dissolved in saline and delivered 1.46 mg/kg/day for 21 days via mini pump. EMD638683 (MedChemExpress, Monmouth Junction, NJ), a selective inhibitor of SGK-1 with no identified alternate targets, was dissolved in dimethylsulfoxide diluted to achieve 2.5 mg/kg/day delivery for 21 days via minipump. Minipump implantation has been previously described.[4,13] Briefly, after the induction of anesthesia, mice underwent subcutaneous left flank implantation of loaded Alzet osmotic mini pump (model 1004; Durect Corporation, Cupertino, CA) to deliver AngII (C57Bl/6+AngII), EMD638683 (C57Bl/6+EMD), or both treatments simultaneously (C57Bl/6+AngII+EMD).

**Blood pressure measurement.** Mouse blood pressures were measured on day 0 and day 21 of treatment. CODA8 tail-cuff method (Kent Scientific, Torrington, CT) was used as previously described.[13,14] Briefly, mice were allowed 10 minutes of acclimation to the chamber. A dark and warm environment was maintained throughout data collection with a heating pad and towel cloak.

**Tissue harvest and processing.** Terminal procedures to image and collect the abdominal aorta were conducted as previously described.[4,13,14] Briefly, mice were anesthetized on day 21 to expose the aorta from the renal vein to the bifurcation. Terminal aortic diameter measurements were taken via calibrated digital microscopy.[4,13,14] Infrarenal aortas were harvested and flash frozen in a liquid nitrogen slurry. Blood from the left ventricle was collected with an EDTA-treated syringe, and centrifuged at 2500$\times g$ for 15 minutes at 4°C. Plasma was harvested and samples were stored in −80°C until further analysis.

**Immunoblot analysis.** Relative abundance of SGK-1, phosphorylated SGK-1 (pSGK-1), and α-tubulin were determined by immunoblotting as previously described.[14,15] Following homogenization of the abdominal aorta, 20 μg of protein was fractionated on a 10% polyacrylamide gel by electrophoresis. The proteins were transferred to nitrocellulose membranes (0.45 μm; Bio-Rad, Hercules, CA) and incubated in antisera specific for SGK-1 (ab32374, AbCam, Waltham, MA; 1:1000), pSGK-1 (ab55281, AbCam; 1:1000), F480 (ab6640, AbCam; 1:1000), and α-tubulin (ab7291, AbCam; 1:1000) in 0.1% Tris-buffered saline with Tween. A secondary peroxidase-conjugated antibody was applied (1:5000; 0.1% Tris-buffered saline with Tween). Signals were detected with a chemiluminescent substrate (Western Lighting Chemiluminescence Reagent Plus; PerkinElmer, San Jose, CA) and recorded on film. Band intensity was quantified using ImageJ 53C software (National Institute of Health, Bethesda, MD).

**Flow cytometry.** Aortic cell harvest for flow cytometric analysis has been previously described.[4,15] Freshly harvested abdominal aorta was minced and placed in Aortic Enzyme Digest Solution (125 U/mL collagenase type XI, 450 U/mL collagenase type I, 60 U/mL DNase-1, and 60 U/mL hyaluronidase type-1-s in 2.5 mL of Dulbecco's phosphate-buffered saline) and incubated at 37°C in 5% $CO_2$ for 2 hours. After digestion, the cells were passed through a 35-μm cell strainer snap cap (352235; Corning Life Sciences, Durham, NC), rinsed with 1 mL BD Pharmingen Stain Buffer (554656; BD Biosciences, San Diego, CA), and centrifuged at 300×*g* at 4°C. The cell pellet was resuspended in 1 mL fluorescence-activated cell sorting buffer, transferred to a new 4-mL snap cap Falcon tube (149,592A; Corning Life Sciences), and centrifuged at 300×*g* at 4°C. Cells were blocked with mouse Fc receptor block (Miltenyi Biotec, San Diego, CA) and stained with conjugated primary antibodies: CD11b-FITC (clone M1/70, BD Biosciences) and F480-BV421 (clone BM8, Biolegends, San Diego, CA) for 20 minutes at 4°C. Cells were then washed, centrifuged at 300×*g* for 10 minutes and resuspended in BD Pharmingen Stain buffer. Cells were fixed by adding 4% formalin/phosphate-buffered saline and incubated for 15 minutes at 23°C. Cells were then washed in BD Pharmingen Stain buffer and centrifuged at 300×*g* and resuspended in BD Pharmingen Stain buffer.

Samples were processed on a CytoFLEX Flow Cytometer (Beckman Coulter, Brea, CA) equipped with CytExpert Software (Beckman Coulter). An average of 100,000 events were recorded for each sample. Analysis of the results was performed using CytExpert software (Version 2.4.0.28, Beckman Coulter). The gating included cell size selection, followed by single cell isolation through side-scatter (Supplementary Fig 1). The remaining events were gated to quantify the percentage of cells with concurrent staining with myeloid marker $CD11b^+$ and the mature macrophage marker $F480^+$.

**Blocking SGK-1 in VSMC culture.** Primary VSMC lines from C57Bl/6 and SGK-$1^{flox+/+}$ abdominal aortas (renal vein to bifurcation) were established using an accepted outgrowth technique as previously described.[16] Isolated VSMCs were maintained in SMC specific growth media with added supplement pack (SMC Growth Medium 2; C-22062, PromoCell, Heidelberg, Germany) at 37°C in 5% $CO_2$. Confirmation of VSMC culture was achieved through western blot analysis demonstrating high levels of alpha-SMA (Supplementary Fig 2).

For SGK-$1^{flox+/+}$ VSMCs that had reached confluency, a kanamycin-resistant Cre-adenovirus (SignaGen, Fredrick, MD) was used to mute transcription of SGK-1 in that subset population. Virus containing media at 100 multiplicity of infection was diluted as recommended and administered to SGK-$1^{flox+/+}$ VSMCs. After 24 hours of infection, cells were treated with kanamycin (Millipore Sigma, Burlington, MA) to remove any nontransfected VSMCs. The abundance of SGK-1 in these VSMCs was confirmed by Western blot to represent approximately a 50% decrease (Supplementary Fig 3); therefore, these were subsequently referred to as SGK-1KD VSMCs. Before use in experimentation, these cells were passaged at least one additional time to allow recovery from the adenovirus and kanamycin treatment.

Confluent C57Bl/6 and SGK-1KD VSMCs from culture passages 2 through 10 were seeded at a density of 5000 cells/$cm^2$ into amino coated Bioflex-6 well plates (BF-3001A; Flexcell International Corporation, Burlington, NC) and allowed to adhere overnight. Complete SMC medium was replaced with serum free SMC basal media (SMC Basal Medium 2; C-22,262, PromoCell) and allowed to rest for 6 hours at 37°C in 5% $CO_2$. VSMCs were treated with with or without EMD638683 (10 μM) and allowed to rest at 37°C in 5% $CO_2$ for 1 hour. After this incubation, plates were held under static conditions (Static) or subjected to 12% biaxial cyclic stretch (Stretch) for 3 hours or 12 hours using the Flexcell culture system (Flexcell International Corporation), as previously described.[4] The rate of Stretch stimulation was 60/min. Cells were harvested to quantify expression of IL-6 and MCP-1 by quantitative polymerase chain reaction (QPCR).

Additionally, small interfering RNA (siRNA) transfection technique was used to silence SGK-1 activity. C57Bl/6 cells were seeded overnight in six-well plates. Reagent containing two SGK-1-specific siRNA (targeting exons 7 and 9) and lipofectamine RNAiMAX cocktail were diluted in culture medium as recommended, as was a silencer select RNA negative control and lipofectamine RNAiMAX cocktail (ThermoFisher, Life Technologies, Carlsbad, CA). Cells were allowed 48 hours incubation in either the SGK-1-specific siRNA transfection media, silencer select transfection media, or control media. Knock-down of

SGK-1 was confirmed to be approximately 70% after treatment with the dual specific siRNA reagent (data not shown). After transfection, cells were lifted and seeded (5000 cells/cm$^2$) overnight on amino-coated Bioflex-6well plate (Flexcell International Corporation) and subjected to Static or Stretch conditions with or without EMD638683 as described elsewhere in this article. Cells were harvested to quantify expression of IL-6 and MCP-1 by QPCR.

**QPCR.** As described previously,[4] after treatment on the Flexcell system, total RNA was extracted using TRIzol Reagent (15596026; Thermo Fisher Scientific, Waltham, MA). One microgram of total RNA was reverse transcribed and converted to complementary DNA (cDNA) using the iScript cDNA synthesis kit (1708891, Bio-Rad). Each cDNA sample was amplified with messenger RNA-specific TaqMan Gene Expression Assays (IL-6, Mm00446190_m1; MCP-1, Mm00441242_m1; GAPDH, Mm99999915_g1; Thermo Fisher Scientific) on a CFX-96 real-time PCR machine (Bio-Rad). Expression values were calculated as $2^{-\Delta\Delta CT}$.

**Enzyme-linked immunosorbent assay.** Enzyme-linked immunosorbent assay (ELISA) was used to quantify the concentration of IL-6 (ab100712; Abcam) and MCP-1 (ab208979; Abcam) in Flexcell treatment conditioned media and murine plasma. Collected cell media was first concentrated using a 10K Centrifugal Filter (UFC201024; Millipore Sigma, Carrigtwohill, CO) and centrifuged at 4000×*g* for 30 minutes at 4°C. The sample recovery was plated in the respective 96-well strip plates. Standard dilution and reagents were prepared in accordance to manufacturer's instructions. Absorbance at 450 nm was measured using a SpectraMax M3 microplate absorbance reading (Molecular Devices, San Jose, CA) with SoftMax Pro (Version 7.1) software.

**Computational modeling.** To explore the role of SGK-1 within the broader cell signaling pathways connecting mechanical stimulation and IL-6 production, we adapted a previously published computational model of VSMC signaling networks.[17-19] Signaling proteins and small molecules included in the network model represent the most well-established pathways connecting AngII and mechanical strain inputs to changes in cell signaling related to IL-6 expression, as well as matrix synthesis (eg, collagens), matrix degradation (eg, matrix metalloproteinases [MMPs]), and cell contractility (eg, actomyosin proteins). These pathways were reconstructed manually based on extensive mechanistic studies in the literature, and the resulting network spans 79 molecules interconnected by 123 reactions including the well-established signaling drivers Akt, Rho, Smads, JNK, ERK, MAPK, p38, mTOR, PI3K, and others. We adapted the previous network by adding SGK-1 reactions supported by previous literature.[20] The full list of integrated species

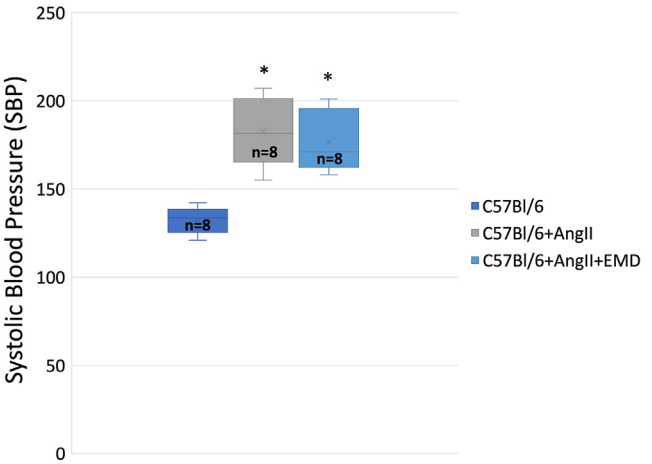


**Fig 1.** Systolic blood pressure as measured by tail cuff. *$P < .05$ vs day 0. *AngII*, Angiotensin II.

and reactions are available as Supplementary Tables I and II.

To simulate the effects of input stimuli on downstream nodes, each connection in the model was simplified as a normalized Hill differential equation according to logic-based gates (AND, OR relationships, Equations 1 and 2):

$$\mathrm{ANDgate}(X+Y\rightarrow Z)\frac{dZ}{dt}=\frac{1}{\tau}\left(\frac{B\cdot X^n}{K^n+X^n}\cdot\frac{B\cdot Y^n}{K^n+Y^n}\cdot Z_{max}-Z\right) \quad \text{Eq. 1}$$

$$\mathrm{ORgate}(X\rightarrow Z\,\mathrm{or}\,Y\rightarrow Z)\frac{dZ}{dt}=\frac{1}{\tau}\left(\times\left(\frac{B\cdot X^n}{K^n+X^n}+\frac{B\cdot Y^n}{K^n+Y^n}-\left(\frac{B\cdot X^n}{K^n+X^n}\cdot\frac{B\cdot Y^n}{K^n+Y^n}\right)\right)\cdot Z_{max}-Z\right) \quad \text{Eq. 2}$$

where X, Y, and Z are node activation levels, τ is a reaction time constant, and n is the classic Hill coefficient that captures the nonlinearity of each reaction's dose-response curve. B and K are additional parameters describing dose-response features and determined by n and the half-maximal activation concentration, according to the Equations 3 and 4:

$$B=\frac{EC_{50}^n-1}{2EC_{50}^n-1} \quad \text{Eq 3}$$

$$K=(B-1)^{\frac{1}{n}} \quad \text{Eq 4}$$

The system of equations is solved using MATLAB code driven by the open-source, Netflux user interface (https://github.com/saucermanlab/Netflux).[21]

Given specific input inhibition or stimulation, the model calculates resulting changes in the expression of primary outputs (IL-6, extracellular matrix, MMPs, etc). This same logic-based Hill equation approach has been applied across a variety of cell types, including VSMCs, vascular

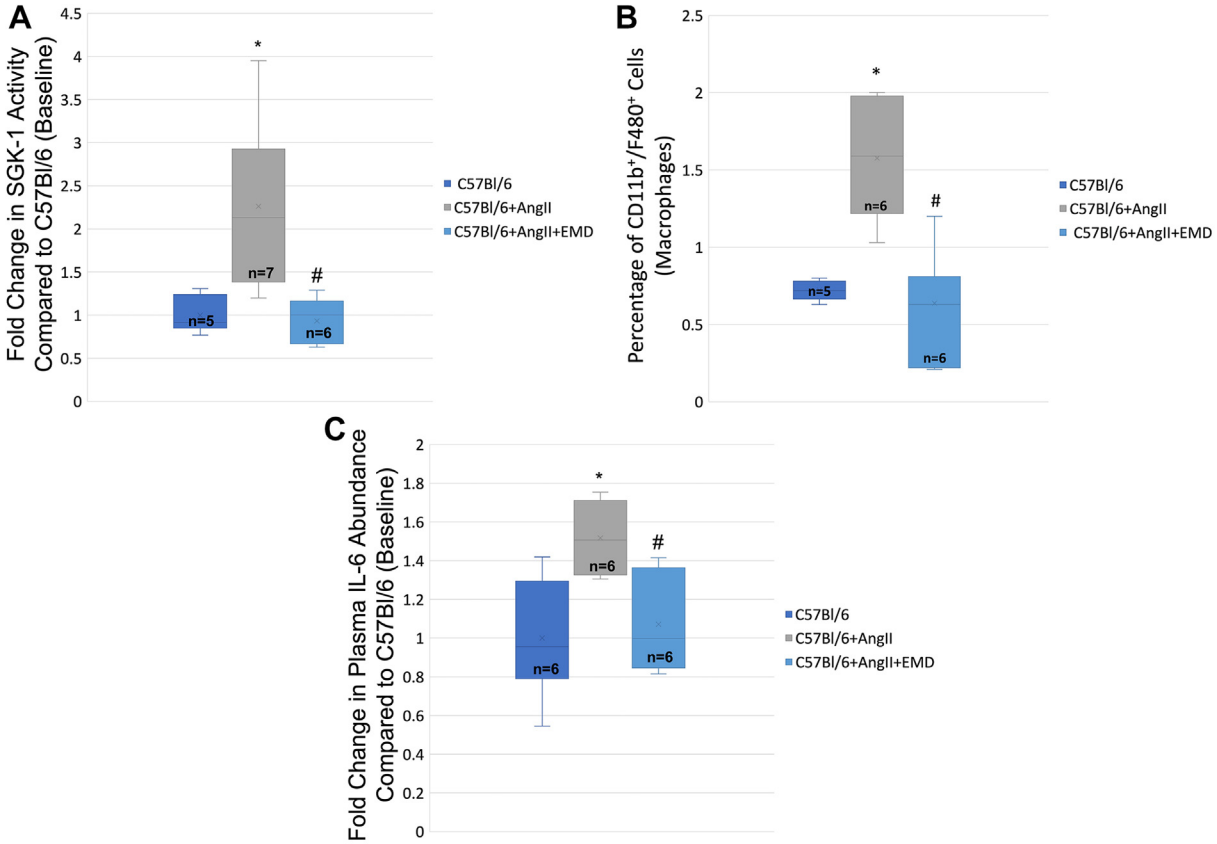


**Fig 2. (A)** SGK-1 activity (pSGK-1/SGK-1) in aortic homogenate at day 21, represented as a fold change from the value in C57Bl/6 control mice (baseline normal physiology). **(B)** Aortic digestion and cell extraction for flow cytometry quantification of $CD11b^{+}/F480^{+}$ cells (macrophages) in abdominal aorta on day 21, presented as a percentage of the total cell complement. **(C)** Quantification of interleukin (*IL*)-6 in plasma of experimental mice at day 21 using ELISA to quantify the protein from the standard curve. Values have been represented as a fold change from the C57Bl/6 control (baseline normal physiology). * $P < .05$ vs C57Bl/6; #$P < .05$ vs C57Bl/6+ angiotensin II (*AngII*).

adventitial fibroblasts, cardiac fibroblasts, valve interstitial cells, macrophages, and cardiomyocytes.[17-19,21-28] Herein, we represented the in vitro experimental conditions by running a baseline control simulation, a heightened mechanical strain simulation, and a strain + SGK-1-inhibition simulation. We represented the in vivo experimental conditions by running a baseline control simulation, a heightened mechanical strain + AngII simulation, and a strain + AngII + SGK-1-inhibition simulation.

**Statistical analysis.** The percent increase in abdominal AoD was calculated as ([terminal AoD − baseline AoD/baseline AoD] × 100 + 100) for each individual mouse. Therefore, the baseline value for each mouse is 100% and the 21-day assessment represents the increase in diameter above baseline. Similar to other investigations into tissue kinase activity,[14,15] SGK-1 activity in the murine aorta was derived as the ratio of the optical density-derived abundance for pSGK-1/SGK-1. This ratio was calculated for each aortic sample and the fold change established relative to the normotensive C57Bl/6 control mice, which represent normal aortic physiology. Similarly, after calculating the cytokine abundance using the ELISA standard curve, the plasma sample from each treatment animal was compared with the normotensive C57Bl/6 control mice to generate a fold change from baseline physiology. Flow cytometric analysis quantified the $CD11b^{+}/F480^{+}$ cells as a percentage of the total cells within the harvested abdominal aortic tissue. QPCR values were assessed as fold change from the wild-type C56Bl/6 Static cells. The conditioned culture media ELISA quantification of IL-6 and MCP-1 was compared with the media from C57Bl/6 Static cells, which represented normal physiology.

Normality of the data was assessed by the D'Agostino-Pearson test for skewness and kurtosis, and each component of the in vivo data was normally distributed. The VSMC cytokine expression data was normally distributed after transformation by log10 and then analyzed with parametric statistics. Culture media data were also normally distributed. In each data set, the groups were compared by analysis of variance with interactions and

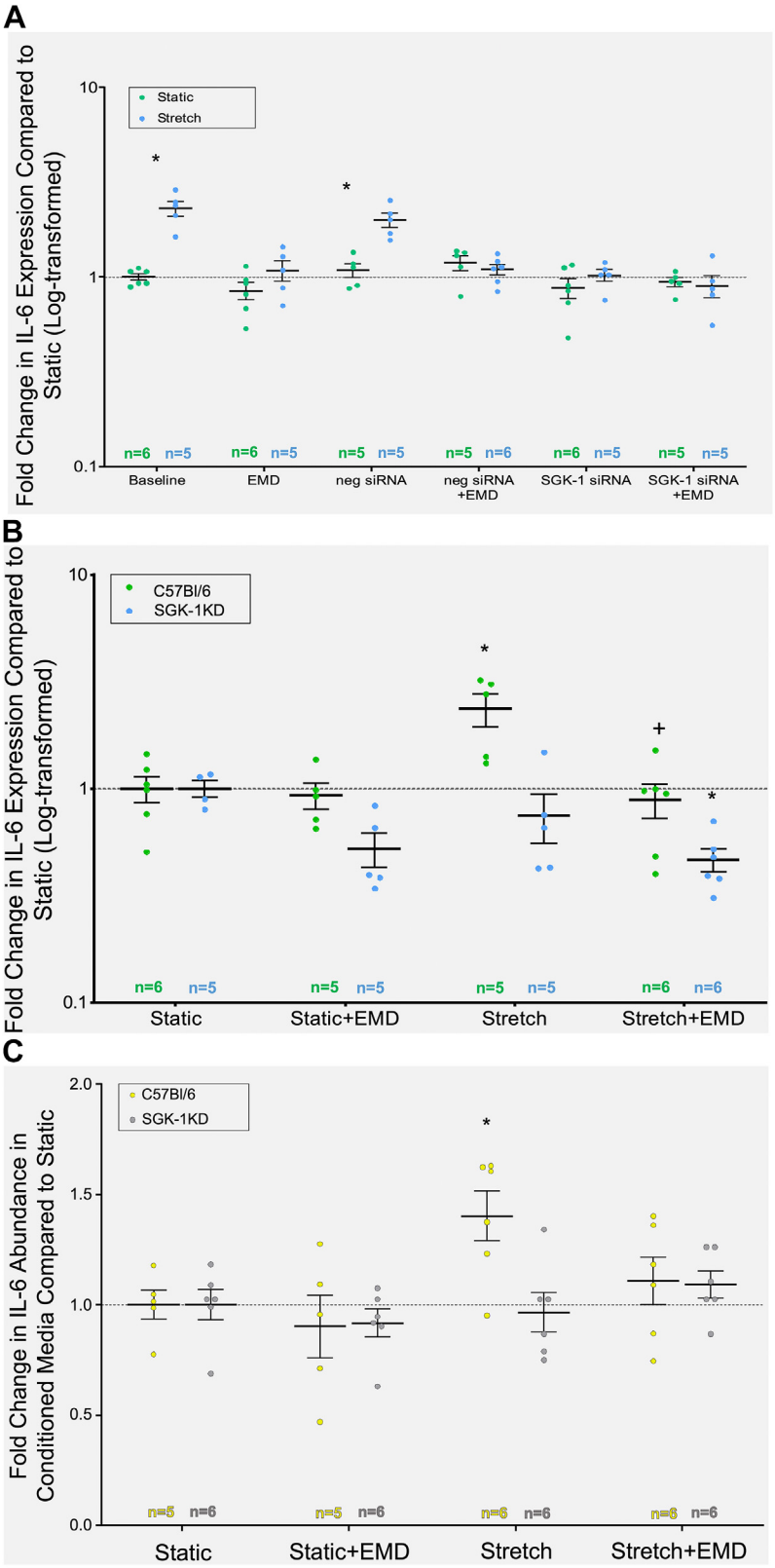


**Fig 3. (A)** Interleukin (*IL*)-6 expression in C57Bl/6 vascular smooth muscle cells (*VSMCs*) treated with or without Stretch, with or without small interfering RNA (*siRNA*), and with or without EMD for 3 hours, represented as a fold change from the C57Bl/6 Static VSMCs (baseline). **(B)** IL-6 expression in C57Bl/6 and SGK-1KD VSMCs treated for 12 hours with or without Stretch and with or without EMD, represented as a fold change from the C57Bl/6 Static VSMCs (baseline). Data in **(A)** and **(B)** graphed and statistically analyzed after log10 transformation. **(C)** IL-6

post hoc mean separation was performed using the Sidak correction for multiple comparisons. Statistical tests were performed using Stata (v17.0, College Station, TX) with significance established at a $P$ value of $<.05$.

## RESULTS

In C57Bl/6 wild-type mice, AngII infusion caused a significant increase in systolic blood pressure (SBP) at 21 days, which was not impacted by EMD treatment (Fig 1). Consistent with prior use of this model in wild-type mice, at terminal procedure neither aortic dilation nor dissection was apparent (data not shown). Abdominal aortic tissue from C57Bl/6+AngII mice demonstrated significant elevations in SGK-1 activity and macrophage infiltration ($P < .05$ vs C57Bl/6), which were effectively inhibited by EMD infusion ($P < .05$ vs C57Bl/6+AngII) (Fig 2, *A* and *B*). Although plasma levels of MCP-1 were not detectable, IL-6 was increased by >1.5 fold ($P < .05$ vs C57Bl/6) and significantly reduced by EMD ($P < .05$ vs C57Bl/6+AngII) (Fig 2, *C*). It has been well-documented that even patients with controlled HTN can develop end-organ damage; therefore, these results suggest that blocking SGK-1 activity and downstream inflammatory markers may represent a complementary treatment paradigm to combat the impact of macrophage-derived proteases on hypertensive vascular pathology.

In C57Bl/6 aortic VSMCs, Stretch led to significant increase in IL-6 and MCP-1 expression ($P < .05$ vs Static) (Figs 3, *A*, and 4, *A*), which was inhibited by treatment with EMD or SGK-1siRNA ($P < .05$ vs Stretch). Dual therapy, however, did not have an additive effect. No response was observed for SGK-1KD VSMCs under Stretch conditions (Fig 3, *B*). IL-6 expression in C57Bl/6 VSMCs and secretion of IL-6 into the culture media followed the same pattern of Stretch-induced elevation with EMD inhibition (Fig 3, *C*). Interestingly, when Stretch was extended to 12 hours, MCP-1 expression in C57Bl/6 cells trended back to baseline Static levels to suggest a negative feedback system to quench transcription. Translational activity continued, however, and the MCP-1 protein abundance in the culture media was significantly elevated ($P < .05$ vs C57Bl/6 Static) (Figs 4, *B* and *C*). In the SGK-1KD VSMCs, the apparent negative feedback decreased MCP-1 expression with Stretch or EMD treatment. Integrating this isolated VSMC data with the murine AngII-induced HTN model may support that mechanical activation of SGK-1 in aortic VSMCs can promote IL-6 production to increase serum levels as well as local tissue MCP-1 levels to contribute to increased macrophage abundance and hypertensive aortic pathology.

Prior experimentation had indicated that adding AngII treatment to mechanical stretch in murine aortic VSMCs did not amplify IL-6 expression beyond that of stretch alone[4]; therefore, dual stimulation concurrent with SGK-1 inhibition was unlikely to strengthen the clinical relevance of this project. Instead, we chose to use computational modeling of VSMC signaling to further evaluate SGK-1 as a major contributor to tension-induced proinflammatory signaling in HTN. Signaling proteins and small molecules included in the VSMC network model (Fig 5, *A*) represent the most well-established pathways connecting AngII and mechanical strain inputs to changes in cell expression related to inflammation (eg, IL-6), matrix synthesis (eg, collagens), degradation (eg, MMPs), and cell contractility (eg, actomyosin proteins). Importantly, the network has included major feedback loops driven by IL-6, and SGK-1 represented a central hub connecting both AngII and mechanical strain inputs to inflammatory, synthetic, degradation, and contractility outputs. Several pertinent positive (Fig 5, *B*) and negative (Fig 5, *C*) feedback loops were observed. Notably, inhibiting SGK1 could interrupt at least three positive feedback loops that may drive IL-6 expression in aortic VSMCs:

$$\mathrm{IL-6} \rightarrow \mathrm{JAK} \rightarrow \mathrm{PI3K} \rightarrow \mathrm{PDK1} \rightarrow \mathbf{SGK-1} \rightarrow \mathrm{NFkB} \rightarrow \mathrm{IL-6}.$$

$$\mathrm{IL-6} \rightarrow \mathrm{JAK} \rightarrow \mathrm{PI3K} \rightarrow \mathrm{PDK1} \rightarrow \mathrm{Akt} \rightarrow \mathrm{mTOR} \rightarrow \mathrm{mTORC2} \rightarrow \mathbf{SGK-1} \rightarrow \mathrm{NFkB} \rightarrow \mathrm{IL-6}.$$

$$\mathbf{SGK-1} \rightarrow \mathrm{TSC12} \rightarrow \mathrm{mTORC2} \rightarrow \mathrm{PI3K} \rightarrow \mathrm{PDK1} \rightarrow \mathbf{SGK-1}.$$

Concordantly, the computational simulations were able to replicate our in vitro findings that inhibition of SGK-1 activity led to a decrease in expression of IL-6 (Fig 5, *D*). The integration of these in vivo, in vitro, and computational data strongly support SGK-1 as a major mechanosensitive kinase in hypertensive vascular pathology.

## DISCUSSION

Moving beyond the role of SGK-1 in renal salt secretion, this project has demonstrated that, in HTN, the mechanical activation of SGK-1 in aortic VSMCs can promote proinflammatory cytokine production and macrophage accumulation as potential contributors to hypertensive aortic pathology. In the AngII-induced HTN model, inhibiting SGK-1 with continuous infusion

abundance in conditioned culture media from C57Bl/6 and SGK-1KD VSMCs treated for 12 hours with or without Stretch and with or without EMD. Abundance values were obtained from the enzyme-linked immunosorbent assay (ELISA) standard curve and represented as a fold change from the C57Bl/6 Static VSMC culture media (baseline). * $P < .05$ vs wild-type (WT) Static, + $P < .05$ vs WT Stretch.

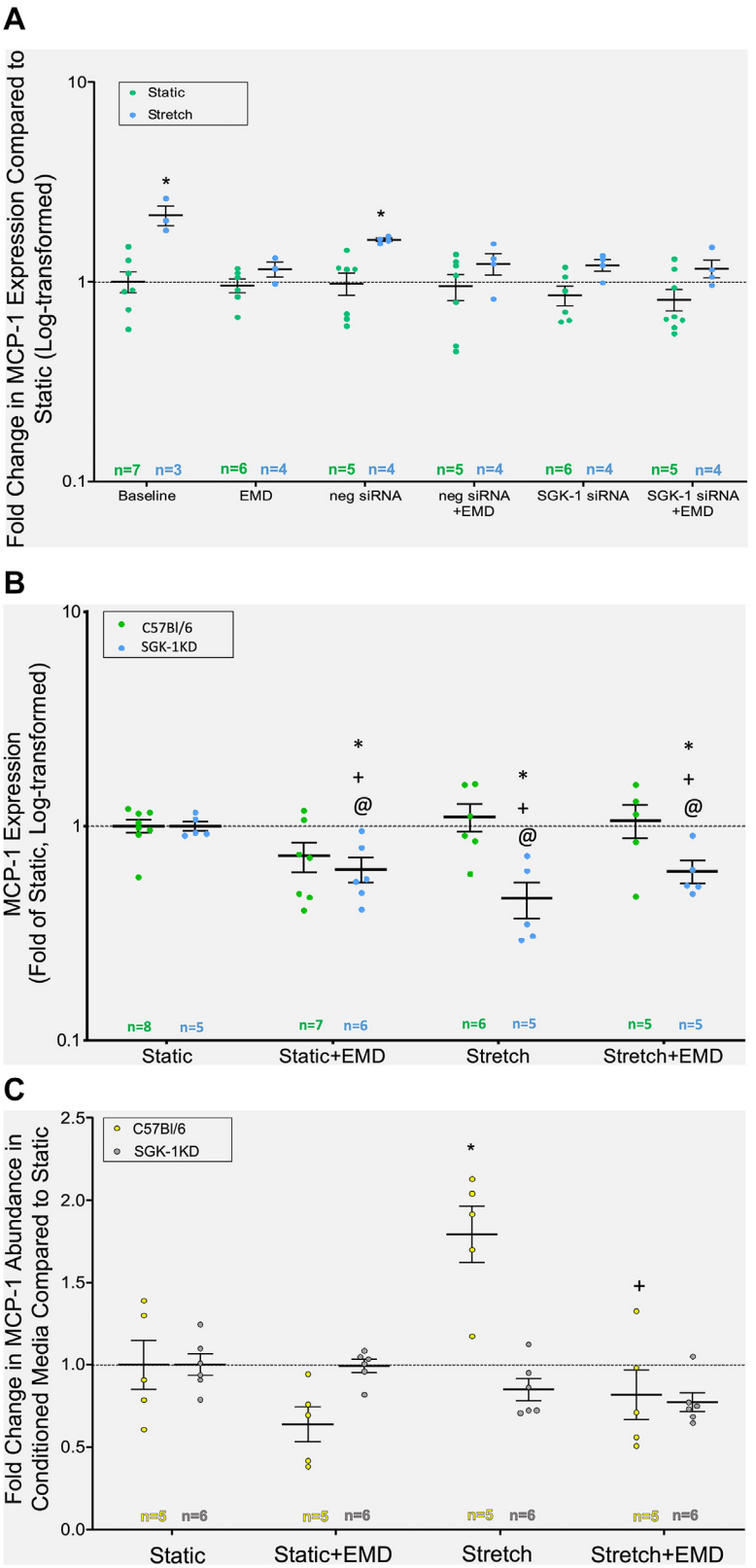


**Fig 4. (A)** MCP-1 expression in C57Bl/6 vascular smooth muscle cells (VSMCs) treated with or without Stretch, with or without small interfering RNA (siRNA), and with or without EMD for 3 hours, represented as a fold change from the C57Bl/6 Static VSMCs (baseline). **(B)** MCP-1 expression in C57Bl/6 and SGK-1KD VSMCs treated for 12 hours with or without Stretch and with or without EMD, represented as a fold change from the C57Bl/6 Static VSMCs (Baseline). [Data in A and B graphed and statistically analyzed following log10 transformation.] **(C)** Monocyte

of EMD638683 did not effect SBP, but significantly reduced plasma IL-6 as well as macrophage infiltration to demonstrate that, despite the ongoing mechanical stimulus, intracellular SGK-1 inhibition decreased inflammatory signaling. The influence of mechanical activation of SGK-1 on cytokine production was further established in harvested murine aortic VSMCs wherein cyclic Stretch fostered IL-6 and MCP-1 expression as well as protein secretion, but this was inhibited with pharmacological or genetic blockade of SGK-1 activity. Furthermore, computational modeling of VSMC signaling owing to mechanical strain and/or AngII stimulation identified pertinent positive feedback loops centered on SGK-1 to upregulate IL-6 expression. Considering the micro- and macrovascular impact of hypertensive pathology, targeting SGK-1 to reduce proinflammatory signaling may represent a vital adjunct to standard antihypertensive therapies.

HTN has been recognized as an inflammatory process, with even mild elevations in blood pressure associated with increased circulating IL-6 levels in otherwise healthy patients.[29,30] Unfortunately, only approximately 30% of patients reach designated blood pressure goals through medical therapy, and evidence suggests that even those who successfully obtain normotension will still have vascular functional abnormalities.[31,32] Notable consequences of inadequately treated HTN include aortic stiffening and left ventricular hypertrophy,[33] both of which represent an increased risk for cardiovascular morbidity and mortality.[34,35] These tension-induced pathologies are driven by inflammatory cell accumulation with protease production and dysfunctional matrix remodeling,[36,37] and indicate that the interruption of cardiovascular mechanotransduction may represent a vital treatment pathway in HTN.

Blockade of SGK-1 activity has been shown to reduce fibrosis in other vascular beds by reduced signaling through nuclear factor κB (NF-κB),[5,6,38] a transcription factor known to influence expression of proinflammatory cytokines such as IL-6 and MCP-1[39]; therefore, our interest focused on SGK-1 as a mediator between mechanical aortic wall tension and inflammatory signaling. In this AngII-induced model of HTN in C57Bl/6 wild-type mice fed standard chow, aortic dissection and aneurysmal degeneration did not occur, but the elevated SBP did correspond with upregulated SGK-1 activity, increased circulating IL-6, and the accumulation of macrophages within the abdominal aortic wall. Because macrophages are major producers of proteases,[40] their abundance represents the potential for pathologic matrix remodeling. Interestingly, despite no change in blood pressure, treatment with EMD638683 decreased SGK-1 activity in parallel with decreased IL-6 levels and fewer macrophages, indicating that mechanical signaling was ongoing but the pathway toward inflammation was disrupted. The computational signaling network further supported this concept because inhibiting SGK-1 disconnected three major positive feedback loops that promote IL-6 expression. Targeting SGK-1 has significant therapeutic implications such that interrupting mechanical signaling as an adjunct to standard antihypertensive drugs may attenuate vascular pathology to reduce end-organ damage and warrants further investigation.

Because SGK-1 is ubiquitously expressed but the response to extracellular stress has been cell-type dependent,[6] it was imperative to isolate murine abdominal aortic VSMCs to demonstrate that, by using pharmacological blockade, silencing RNA, and genetic knockout, this tension-induced cytokine production was SGK-1 dependent. Interestingly, despite the increase in MCP-1 expression and secretion in VSMCs under Stretch conditions, circulating levels of this cytokine were undetectable in the mice with AngII-induced HTN, raising a possibility that MCP-1 acted in a paracrine fashion within the aortic wall to promote macrophage accumulation. Alternatively, the production and secretion of IL-6 from aortic VSMCs likely represented a source for the elevated circulating IL-6 levels noted in vivo; therefore, mechanical activation of SGK-1 in aortic VSMCs promoted local and systemic inflammation. The computational network provided further evidence of integrated signaling by mechanical strain and AngII in aortic VSMCs with SGK-1 serving as a major hub for upregulation of IL-6 expression. As noted in the computational signaling network, NF-κB has been a known target for SGK-1 in VMSCs and can influence expression of both IL-6 and MCP-1.[41,42] Interestingly, however, MCP-1 expression trended back to baseline with prolonged stimulation, whereas IL-6 remained elevated, suggesting that negative feedback systems differentially impacted tension-induced cytokine expression. This observation corresponds with the pro- and anti-inflammatory effects reported for NF-κB and highlights the challenge of therapeutically targeting this transcription factor without undesirable side effects.[43] With the concurrent evidence relating SGK-1 activity to VSMC proliferation, migration, and calcification based on alternative extracellular stressors such as glucose, adipokines, phosphates, and growth factors,[41,42,44-46] integrating the impact of mechanical

chemoattractant protein-1 (*MCP-1*) abundance in conditioned culture media from C57Bl/6 and SGK-1KD VSMCs treated for 12 hours with or without Stretch and with or without EMD. Abundance values were obtained from the enzyme-linked immunosorbent assay (ELISA) standard curve and represented as a fold change from the C57Bl/6 Static VSMC culture media (baseline). *$P < .05$ vs wild-type (WT) Static; +$P < .05$ vs WT Stretch; @$P < .05$ vs SGK-1KO Static.

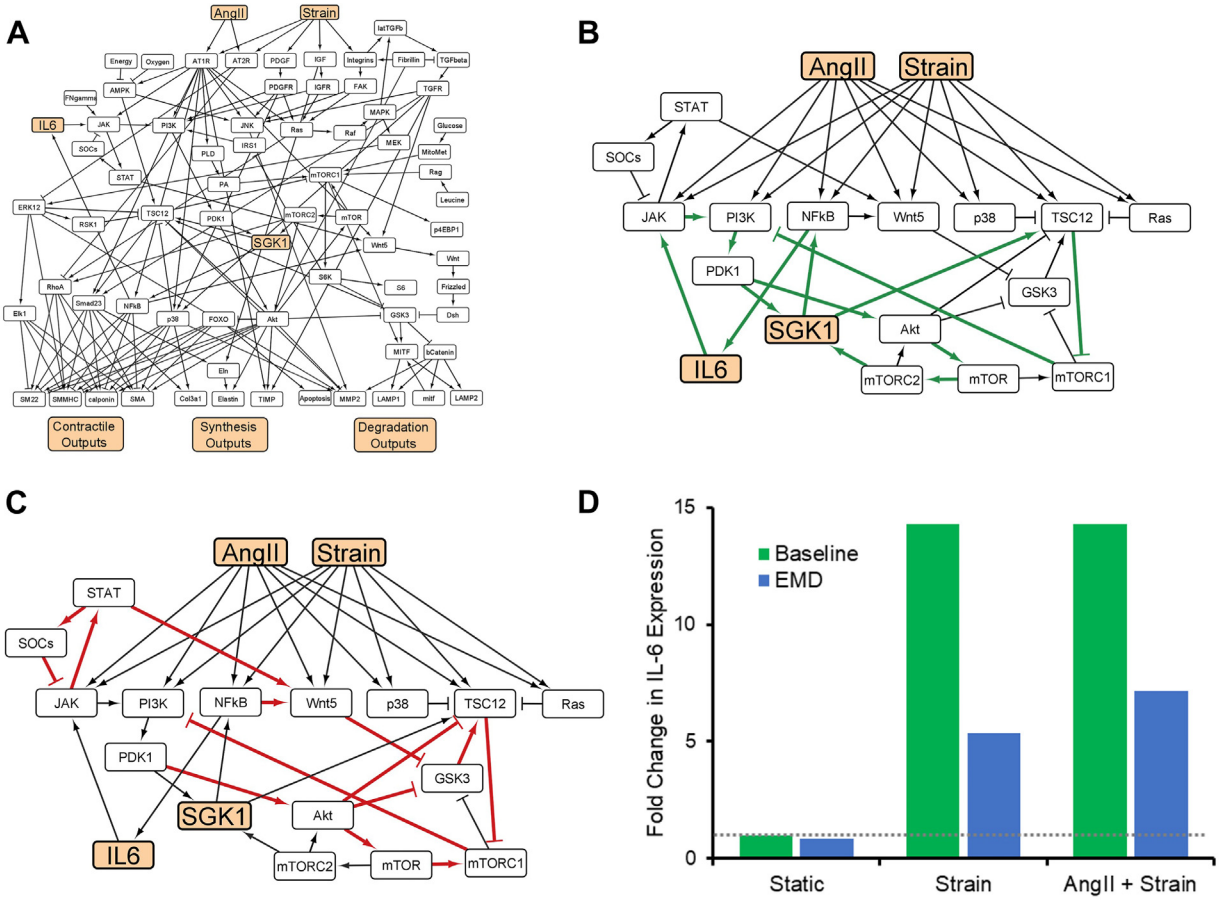


**Fig 5. (A)** A network model of smooth muscle cell (SMC) signaling enabling quantitative, differential equation-based predictions of cell expression responses to angiotensin II (*AngII*) and mechanical strain. **(B, C)** Further, a simplified model topology identified negative feedback loops **(B)** and positive feedback loops **(C)** that contribute to the complexity of interleukin (*IL*)-6 regulation. **(D)** Model prediction that inhibiting SGK-1 activity with EMD638683 will result in a substantial reduction of IL-6 expression in vascular SMCs (*VSMCs*) under mechanical and AngII treatments.

activation on inflammatory cell infiltration further demonstrates the value of pharmacologically inhibiting SGK-1 to abrogate vascular pathology.

**Limitations.** Having demonstrated that tension-induced cytokine expression can be SGK-1 dependent and may represent a viable target to decrease dysfunctional hypertensive vascular inflammatory signaling, this project does have several limitations. First, although several prior studies have used salt-induced animal models of HTN to evaluate SGK-1, we chose to use the AngII-induced murine HTN model for the benefit of its parallelism with the human condition. This model also allows subsequent integration of angiotensin-converting enzyme inhibitors or angiotensin receptor blockers to determine how those medications influence SGK-1 activity and potential benefit for dual therapy with an SGK-1 inhibitor. Second, this project used a single in vivo HTN timepoint and cannot comment on the effect of longer term uncontrolled HTN or pharmacologically corrected SBP on aortic inflammation, but future studies may incorporate that experimental group. Third, having previously demonstrated that AngII exposure to Static murine aortic VSMCs did not significantly increase expression of IL-6 or MCP-1, and that concurrent treatment with AngII and Stretch had no additive effect over Stretch alone,[4] we chose not to repeat all of those experiments with the SGK-1 inhibitor. This decision was further supported by the symmetry of the in vitro and in vivo models, but may be revisited in future studies using antihypertensive medications to identify vital agents in VSMC mechanotransduction for SGK-1 activity. Finally, our computational modeling focused on the contributors to IL-6 expression since this was reflected in the in vivo murine experimentation, but interrogation of major signaling nodes will be influential in determining efficacy and safety of SGK-1 inhibition. Future investigation may also explore the signaling network specific to MCP-1 and its relationship to macrophage accumulation.

## CONCLUSIONS

Mechanical activation of SGK-1 in aortic VSMCs can promote inflammatory signaling and increased macrophage abundance; therefore, this kinase warrants further exploration as a pharmacotherapeutic target to abrogate hypertensive vascular pathology.

## AUTHOR CONTRIBUTIONS

Conception and design: RM, JJ, JR
Analysis and interpretation: MF, VM, YX, RM, WR, JR
Data collection: MF, SH, VM, AM, AB, YX, WR, JR
Writing the article: MF, SH, VM, AM, AB, YX, JR
Critical revision of the article: MF, YX, RM, JJ, WR, JR
Final approval of the article: MF, SH, VM, AM, AB, YX, RM, JJ, WR, JR
Statistical analysis: MF, RM, JR
Obtained funding: MF, AB, JJ, JR
Overall responsibility: JR

## DISCLOSURES

J.M.R. is a surgical proctor for CVRx, outside the scope of the submitted work.

## REFERENCES

1. Haga JH, Li YS, Chien S. Molecular basis of the effects of mechanical stretch on vascular smooth muscle cells. J Biomech 2007;40:947-60.
2. Anwar MA, Shalhoub J, Lim CS, Gohel MS, Davies AH. The effect of pressure-induced mechanical stretch on vascular wall differential gene expression. J Vasc Res 2012;49:463-78.
3. Harrison DG, Marvar PJ, Titze JM. Vascular inflammatory cells in hypertension. Front Physiol 2012;3:128.
4. Akerman AW, Stroud RE, Barrs RW, et al. Elevated wall tension initiates interleukin-6 expression and abdominal aortic dilation. Ann Vasc Surg 2018;46:193-204.
5. Cheng J, Wang Y, Ma Y, et al. The mechanical stress-activated serum-, glucocorticoid-regulated kinase 1 contributes to neointima formation in vein grafts. Circ Res 2010;107:1265-74.
6. BelAiba RS, Djordjevic T, Bonello S, et al. The serum- and glucocorticoid-inducible kinase Sgk-1 is involved in pulmonary vascular remodeling: role in redox-sensitive regulation of tissue factor by thrombin. Circ Res 2006;98:828-36.
7. Xi X, Liu S, Shi H, et al. Serum—glucocorticoid regulated kinase 1 regulates macrophage recruitment and activation contributing to monocrotaline-induced pulmonary arterial hypertension. Cardiovasc Toxicol 2014;14:368-78.
8. Lang F, Huang DY, Vallon V. SGK, renal function and hypertension. J Nephrol 2010;23(Suppl 16):S124-9.
9. Van Beusecum JP, Barbaro NR, McDowell Z, et al. High salt activates CD11c $^{+}$ Antigen-Presenting cells via SGK (serum glucocorticoid kinase) 1 to promote renal inflammation and salt-sensitive. Hypertension 2019;74:555-63.
10. Norlander AE, Saleh MA, Pandey AK, et al. A salt-sensing kinase in T lymphocytes, SGK1, drives hypertension and hypertensive end-organ damage. JCI Insight 2017;2:e92801.
11. Lima RSd, Silva JCdS, Lima CT, et al. Proinflammatory role of angiotensin II in the aorta of normotensive mice. Biomed Res Int 2019;2019:1-11.
12. Fejes-Toth G, Frindt G, Naray-Fejes-Toth A, Palmer LG. Epithelial Na+ channel activation and processing in mice lacking SGK1. Am J Physiol Renal Physiol 2008;294:F1298-305.
13. Ruddy JM, Akerman AW, Kimbrough D, et al. Differential hypertensive protease expression in the thoracic versus abdominal aorta. J Vasc Surg 2017;66:1543-52.
14. Hall S, Ward ND, Patel R, et al. Mechanical activation of the angiotensin II type 1 receptor contributes to abdominal aortic aneurysm formation. JVS Vasc Sci 2021;2:194-206.
15. Patel R, Hall S, Lanford H, et al. Signaling through the IL-6-STAT3 pathway promotes proteolytically-active macrophage accumulation necessary for development of small AAA. Vasc Endovascular Surg 2023;57:433-44.
16. Ray JL, Leach R, Herbert JM, Benson M. Isolation of vascular smooth muscle cells from a single murine aorta. Methods Cell Sci 2001;23:185-8.
17. Estrada AC, Irons L, Rego BV, Li G, Tellides G, Humphrey JD. Roles of mTOR in thoracic aortopathy understood by complex intracellular signaling interactions. PLoS Comput Biol 2021;17:e1009683.
18. Irons L, Humphrey JD. Cell signaling model for arterial mechanobiology. PLoS Comput Biol 2020;16:e1008161.
19. Irons L, Latorre M, Humphrey JD. From transcript to tissue: multiscale modeling from cell signaling to matrix remodeling. Ann Biomed Eng 2021;49:1701-15.
20. Zhu R, Yang G, Cao Z, et al. The prospect of serum and glucocorticoid-inducible kinase 1 (SGK1) in cancer therapy: a rising star. Ther Adv Med Oncol 2020;12:175883592094094.
21. Kraeutler MJ, Soltis AR, Saucerman JJ. Modeling cardiac β-adrenergic signaling with normalized-hill differential equations: comparison with a biochemical model. BMC Syst Biol 2010;4:157.
22. Ryall KA, Holland DO, Delaney KA, Kraeutler MJ, Parker AJ, Saucerman JJ. Network reconstruction and systems analysis of cardiac myocyte hypertrophy signaling. J Biol Chem 2012;287:42259-68.
23. Liu X, Zhang J, Zeigler AC, Nelson AR, Lindsey ML, Saucerman JJ. Network analysis reveals a distinct axis of macrophage activation in response to conflicting inflammatory cues. J Immunol 2021;206:883-91.
24. Tan PM, Buchholz KS, Omens JH, McCulloch AD, Saucerman JJ. Predictive model identifies key network regulators of cardiomyocyte mechano-signaling. PLoS Comput Biol 2017;13:e1005854.
25. Zeigler AC, Richardson WJ, Holmes JW, Saucerman JJ. A computational model of cardiac fibroblast signaling predicts context-dependent drivers of myofibroblast differentiation. J Mol Cell Cardiol 2016;94:72-81.
26. Rogers JD, Richardson WJ. Fibroblast mechanotransduction network predicts targets for mechano-adaptive infarct therapies. Elife 2022;11:e62856.
27. Rogers JD, Aguado BA, Watts KM, Anseth KS, Richardson WJ. Network modeling predicts personalized gene expression and drug responses in valve myofibroblasts cultured with patient sera. Proc Natl Acad Sci U S A 2022;119:e2117323119.
28. Wang A, Cao S, Aboelkassem Y, Valdez-Jasso D. Quantification of uncertainty in a new network model of pulmonary arterial adventitial fibroblast pro-fibrotic signalling. Phil Trans Math Phys Eng Sci 2020;378:20190338.
29. Chae CU, Lee RT, Rifai N, Ridker PM. Blood pressure and inflammation in apparently healthy men. Hypertension 2001;38:399-403.
30. Chamarthi B, Williams GH, Ricchiuti V, et al. Inflammation and hypertension: the interplay of interleukin-6, dietary sodium, and the renin-angiotensin system in humans. Am J Hypertens 2011;24:1143-8.
31. Liu K, Colangelo LA, Daviglus ML, et al. Can antihypertensive treatment restore the risk of cardiovascular disease to ideal levels?: The coronary artery risk development in young adults (CARDIA) study and the multi-ethnic study of atherosclerosis (MESA). J Am Heart Assoc 2015;4:e002275.
32. Ticcinelli V, Stankovski T, Iatsenko D, et al. Coherence and coupling functions reveal microvascular impairment in treated hypertension. Front Physiol 2017;8:749.
33. Laurent S, Briet M, Boutouyrie P. Large and small artery cross-talk and recent morbidity-mortality trials in hypertension. Hypertension 2009;54:388-92.
34. Garg P, Assadi H, Jones R, et al. Left ventricular fibrosis and hypertrophy are associated with mortality in heart failure with preserved ejection fraction. Sci Rep 2021;11:617.
35. Laurent S, Boutouyrie P, Asmar R, et al. Aortic stiffness is an independent predictor of all-cause and cardiovascular mortality in hypertensive patients. Hypertension 2001;37:1236-41.
36. Zanoli L, Boutouyrie P, Fatuzzo P, et al. Inflammation and aortic stiffness: an individual participant data meta-analysis in patients with inflammatory bowel disease. J Am Heart Assoc 2017;6:e007003.
37. Gan W, Ren J, Li T, et al. The SGK1 inhibitor EMD638683, prevents Angiotensin II-induced cardiac inflammation and fibrosis by blocking NLRP3 inflammasome activation. Biochim Biophys Acta 2018;1864:1-10.

38. Lang F, Artunc F, Vallon V. The physiological impact of the serum and glucocorticoid-inducible kinase SGK1. Curr Opin Nephrol Hypertens 2009;18:439-48.
39. Zhong Y, Liu C, Feng J, Li JF, Fan ZC. Curcumin affects ox-LDL-induced IL-6, TNF-α, MCP-1 secretion and cholesterol efflux in THP-1 cells by suppressing the TLR4/NF-κB/miR33a signaling pathway. Exp Ther Med 2020;20:1856-70.
40. Ruddy JM, Ikonomidis JS, Jones JA. Multidimensional contribution of matrix metalloproteinases to atherosclerotic plaque vulnerability: multiple mechanisms of inhibition to promote stability. J Vasc Res 2016;53:1-16.
41. Poetsch F, Henze LA, Estepa M, et al. Role of SGK1 in the osteogenic transdifferentiation and calcification of vascular smooth muscle cells promoted by hyperglycemic conditions. Int J Mol Sci 2020;21:7207.
42. Voelkl J, Luong TTD, Tuffaha R, et al. SGK1 induces vascular smooth muscle cell calcification through NF-κB signaling. J Clin Invest 2018;128:3024-40.
43. Liu D, Zhong Z, Karin M. NF-κB: a double-edged sword controlling inflammation. Biomedicines 2022;10:1250.
44. Walker-Allgaier B, Schaub M, Alesutan I, et al. SGK1 up-regulates orai1 expression and VSMC migration during neointima formation after arterial injury. Thromb Haemost 2017;117:1002-5.
45. Scott TA, Babayeva O, Banerjee S, Zhong W, Francis SC. SGK1 is modulated by resistin in vascular smooth muscle cells and in the aorta following diet-induced obesity. Obesity 2016;24:678-86.
46. Zhong W, Oguljahan B, Xiao Y, et al. Serum and glucocorticoid-regulated kinase 1 promotes vascular smooth muscle cell proliferation via regulation of beta-catenin dynamics. Cell Signal 2014;26:2765-72.

Submitted Dec 27, 2022; accepted Aug 1, 2023.